

# Amphiphilogs for Drug Delivery: Formulation and Characterization

Nadeen Jibry,<sup>1</sup> Richard K. Heenan,<sup>2</sup> and Sudaxshina Murdan<sup>1,3</sup>

Received May 20, 2004; accepted June 28, 2004

**Purpose.** This study examines the microstructure, gelation temperatures, and flow properties of novel amphiphilogs consisting solely of non-ionic surfactants.

**Methods.** Gels were prepared by mixing the solid gelator (sorbitan monostearate or sorbitan monopalmitate) and the liquid phase (liquid sorbitan esters or polysorbates) and heating them at 60°C to form a clear isotropic sol phase, and cooling the sol phase to form an opaque semisolid at room temperature. Gel microstructure was examined by light and electron microscopy and by small angle neutron scattering (SANS); gelation temperatures were measured by hot-stage microscopy, a melting point apparatus, and high sensitivity differential scanning calorimetry (HSDSC). Flow rheograms were performed to establish the zero-rate viscosity of the gels and their performance under shear.

**Results.** Gel microstructures consisted mainly of clusters of tubules of gelator molecules that had aggregated upon cooling of the sol phase, forming a 3D network throughout the continuous phase. The gels demonstrated thermoreversibility. Gelation temperature and viscosity increased with increasing gelator concentration, indicating a more robust gel network. At temperatures near the skin surface temperature, the gels softened considerably; this would allow topical application.

**Conclusions.** This study has demonstrated the formation/preparation of stable, thermoreversible, thixotropic surfactant gels (amphiphilogs) with suitable physical properties for topical use.

**KEY WORDS:** amphiphilogs; gelation temperature; nonionic surfactants; SANS; viscosity.

## INTRODUCTION

The gel state has been defined in many different ways (1); Hermans defined the gel as a colloid disperse system that is solid-like in its mechanical properties and which consists of at least two components that extend themselves continuously throughout the whole system (2). Later, Flory added that a gel must have a continuous structure, for example, well-ordered lamellar structures, disordered physically aggregated polymer networks, covalent polymeric networks, particulate structures (3). The gel state can be further classified depending on the nature of the bonds involved in the three-dimensional solid network, as well as on the nature of the

liquid phase. Thus, chemical gels arise when strong covalent bonds hold the network together and physical gels when the hydrogen bonds and electrostatic and van der Waals interactions maintain the gel network (2). When the liquid component is aqueous, the gel is termed a hydrogel and when the liquid is an organic medium, the gel is called an organogel. In our laboratories, we have formulated novel organogels where the liquid phase is a surfactant, and have termed these "amphiphilogs," based on the amphiphilic nature of the fluid phase (4). Interestingly, the gelators are also amphiphiles (sorbitan monostearate or sorbitan monopalmitate) which have previously been reported to gel organic solvents such as hexadecane, sesame seed oil, and isopropyl myristate (5).

The amphiphilogs, where one surfactant causes the gelation of another, are being studied as delivery vehicles for drugs by the oral route. The gels are able to dissolve certain poorly water-soluble drugs such as cyclosporin and can, therefore, be used as vehicles for these "difficult" drugs. *In vivo* experiments in mice and dogs that were orally dosed with cyclosporin-containing gels showed high oral absorption;  $C_{max}$  and  $AUT_{24}$  being similar to those achieved with the commercial preparation Neoral in dogs (6–7). A good bioavailability was related to the fact that the drug did not precipitate out, but stayed in a solubilized form when the gel interacted with the aqueous gastric fluids. The amphiphilogs are also being studied as topical and transdermal carriers for drugs and vaccines; it was thought that the surfactant nature of the gels would enhance permeation of the active agents into and/or through the skin. The fact that the surfactants were nonionic indicated that the gels could be used as topical/transdermal carriers without causing significant irritancy to the skin. Indeed, in experiments in mice and in man, we have shown that the gels, applied twice a day for 5 consecutive days, showed little irritancy to the skin (8).

In this paper, we report on the formation and the physical characterization of amphiphilogs. In an attempt to understand the nature of the gels and their behavior when topically applied to the skin as drug delivery vehicles, gelation temperature, gel lifetime, gel microstructure, and gel rheology were investigated using a number of different techniques.

## MATERIALS AND METHODS

### Materials

The sorbitan esters (Spans) and polysorbates (Tweens) were purchased from Sigma-Aldrich (Dorset, UK) and used as received. These surfactants are usually mixtures, for example, sorbitan monostearate is a mixture of sorbitan esters, with a predominance of stearate ester. Purer protonated sorbitan monostearate (H-Sp60) used for small angle neutron scattering (SANS) was also obtained from Sigma-Aldrich. Deuterated sorbitan monostearate (D-Sp60), also required for the SANS work was synthesized at the Physical and Theoretical Chemistry Laboratories, Oxford University (Oxford, UK). The synthesis involved mixing sorbitol and deuterated stearic acid in a one-step reaction where the sorbitol is dehydrated and esterified in the same reaction vessel, under the influence of an acid catalyst, at 230°C (9–10). The product was tested against commercial nondeuterated Span 60 by TLC.

<sup>1</sup> Department of Pharmaceutics, School of Pharmacy, University of London, London, WC1N 1AX, UK.

<sup>2</sup> ISIS Facility, Rutherford Appleton Laboratory, Didcot, Oxon, OX11 0QX, UK.

<sup>3</sup> To whom correspondence should be addressed. (e-mail: sudax.murdan@ulsop.ac.uk)

**ABBREVIATIONS:** cac, critical aggregation concentration; HSDSC, high sensitivity differential scanning calorimetry; LOQ, low Q neutron beam at the ISIS facility; mgc, minimum gelation concentration; SANS, small angle neutron scattering; T, phase transition temperature.

Distilled water was used whenever required. Deuterated water ( $D_2O$  for SANS) was obtained from Sigma-Aldrich.

### Gel Preparation

Span 40 (sorbitan monopalmitate) and Span 60 (sorbitan monostearate) were used as the gelators (solid component of the gel), and the fluid phases consisted of liquid Spans or liquid Tweens. The solid gelator was weighed into a glass vial and the required amount of liquid surfactant was added. The vial was then placed in a water bath at  $60^\circ\text{C}$  for 10 min with occasional vortexing. The solid gelator dissolved/dispersed in the liquid surfactant and a sol phase (homogenous liquid) was produced. The sol phase was allowed to cool by standing at room temperature overnight. Gelation (defined as the transition from a sol to a gel state) was considered successful, if, upon inversion of the vial, samples did not flow perceptibly. Obviously, this is a crude method of determining whether gelation occurred. This was considered sufficient, however, for screening the large number of samples tested in these studies. Gels will be referred to as  $\chi\%$ Sp/Tw in the text for brevity, for example, 20% w/w Span 60 in Tween 20 will be shortened to 20%Sp60/Tw20.

### Determination of Minimum Gelation Concentration

Gelator/solvent mixtures containing increasing concentrations of gelator were prepared and observed for gel formation. The lowest concentration of gelator which caused gelation at room temperature ( $20^\circ\text{C}$ ) was taken as the minimum gelation concentration.

### Investigation of Gel Microstructure by Light and Electron Microscopy

A thin smear of the gel was placed on a microscope slide, covered with a cover slip, and observed under a Nikon Microphot-FXA (Kanagawa, Japan) light microscope equipped with a Linkham hot-stage and camera (Nikon FX-35DX).

Cryogenic scanning electron microscopy (SEM, Philips XL20, Surrey, UK) was used for higher magnifications. Samples were frozen in liquid nitrogen, the temperature was raised slightly to sublime any condensed water off the surface of the sample which was then coated with gold and viewed under vacuum.

### Investigation of Gel Microstructure by Small Angle Neutron Scattering (SANS)

SANS measurements were carried out on the LOQ instrument at the ISIS pulsed spallation neutron source at the Rutherford Appleton Laboratory (Didcot, UK). Span 60 (either protonated or deuterated) was used as the gelator; Span 80 (H-Sp80), Tween 20 (H-Tw20), and Tween 80 (H-Tw80) were used for the continuous phase of the amphiphilogs. Gels with varying concentrations of H-Sp60 or D-Sp60 were prepared as described earlier. The gels were melted prior to filling into pre-warmed 1-mm path-length HELMA quartz sample cells. The latter were mounted on a sample changer surrounded by a thermostated water bath. SANS profiles were gathered over the  $Q$  range of  $0.006\text{--}0.27\text{ \AA}^{-1}$ , at varying temperatures from  $20^\circ\text{C}$  (room temperature) to  $60^\circ\text{C}$  (above the gel's phase transition temperature). Measuring times of 10 min were used for transmission measurements and a total of

2 h for the scattering determinations. LOQ uses neutrons of wavelengths  $\lambda = 2.2$  to  $10\text{ \AA}$  recorded by time-of-flight, with a 64 cm square detector at 4.1 m from the sample. Scattering vector  $Q = (4\pi/\lambda)\sin(\theta/2)$  where  $\theta$  is the scattering angle. All the scattering data were corrected for instrumental factors, background, sample transmission, and detector efficiencies, and were reduced to absolute values by reference to a standard scatterer (polystyrene blend), to give the scattering cross-section of  $d\Sigma/d\Omega$  [also known as  $I(Q)$ ]. For scattering from dilute particles of uniform composition:

$$I(Q) = \phi(1 - \phi)V(\Delta\vartheta)^2P(Q,R)S(Q,R,\phi) + \text{BKG} \quad (1)$$

where  $\phi$  is the total volume fraction,  $V$  is the volume of one particle,  $\Delta\vartheta$  is the neutron scattering length density difference between the particle and solvent,  $P(Q,R)$  is the form factor for the size and shape of the particle [ $P(Q) \rightarrow 1$  as  $Q \rightarrow 0$ ],  $S(Q)$  is the structure factor for interparticle interactions [for very large and/or dilute particles  $S(Q) \rightarrow 1$ ], and BKG is a generally flat background due to incoherent and inelastic scatter, predominantly from H atoms.

### Determination of Phase Transition Temperatures (T) of Amphiphilogs

The gel-to-sol and/or sol-to-gel phase transition temperatures were measured using three different techniques: melting point apparatus, hot-stage microscopy and by high sensitivity differential scanning calorimetry (HSDSC), as detailed below.

#### By Melting Point Apparatus

A Bibby Stuart Scientific Melting Point SMP1 apparatus was used. The gel was introduced into the capillary tube (100 mm in length and 1.3 to 1.4 mm outer diameter) by dipping the tube into the semisolid to obtain a sample of approximately 0.5 cm in length within the tube. The sample was then drawn up the tube to approximately 0.3 cm from the lower end of the tube using a syringe. The gel-filled tubes were then placed in the melting point apparatus and the temperature was increased by  $1^\circ\text{C}/\text{min}$ . Gel phase transition temperature was taken as the temperature at which the gels melted into an isotropic liquid that flowed down the capillary tube (11). Five samples of each gel were used to obtain an average.

#### By Hot Stage Microscopy

A thin smear of the gel was placed between two cover slips, which were placed on the hot stage light microscope. The temperature of the stage was increased slowly and changes in the gel microstructure were observed. The melting range was taken as the temperature at which the gel structures started to flow to the temperature at which the gel structures melted completely and disappeared. From the melting range, a median was calculated.

By high sensitivity differential scanning calorimetry (HSDSC): A Seteram Micro DSC III high sensitivity differential scanning calorimeter (France) was used to determine the phase transition of some gels. Samples ( $n = 3$ ) of 50–60 mg were weighed into a stainless steel sample cell, heated at a rate of  $1^\circ\text{C}/\text{min}$  from  $0^\circ\text{C}$  to  $60^\circ\text{C}$ , and then cooled down to  $0^\circ\text{C}$  at the same speed, against a blank reference cell. The endothermic peak on the DSC trace, corresponding to the gel to sol phase transition, was used to determine the phase tran-

sition temperature. A blank run where both cells were empty was also conducted under the same conditions, to obtain a baseline.

### Determination of Gel Lifetime

Three samples of each gel were placed in closed glass vials at constant room temperature and observed weekly for any phase separation (syneresis). Gel lifetime was taken as the duration between gel preparation and gel syneresis.

### Determination of Gel Flow Properties Under Continuous Shear Analysis

Flow rheometry of each formulation was performed using the Carri-Med CSL<sup>2</sup>-500 rheometer, in flow mode with a cone-and-plate geometry, and a fixed plate gap of 50  $\mu\text{m}$ . Samples were applied onto the lower stationary plate of the rheometer with a spatula to ensure minimal formulation shearing, and allowed to equilibrate for 15 min prior to analysis. Rheograms were produced under controlled stress by gradually increasing the stress from 0.5 Pa to 500 Pa (or 1000 Pa for harder gels) in a stepped ramp, waiting for equilibrium each time, then returning to the minimum stress in the same manner. Temperature was kept constant at  $25 \pm 0.1^\circ\text{C}$ . Triplicate measurements were performed, using a fresh sample each time, as these measurements are destructive to the gel structure. Zero-rate viscosity was calculated and used for comparison.

The effect of storage on the gels' flow properties was investigated by carrying out the same procedure at 1, 6, 12, and 24 months after gel preparation. To determine the effect of temperature on the flow properties of the gels, the flow procedure was carried out at  $32^\circ\text{C}$  and at  $45^\circ\text{C}$ , with stresses of 0.5 Pa to 200 Pa and back to 0.5 Pa in a stepped ramp.

### Data Analysis

ANOVA was used to analyze the differences in melting points and viscosities of the different gels. Students *t* test was

used to analyze the difference in flow properties following storage.

## RESULTS

### Gel Formation and Minimum Gelation Concentration

Amphiphilogels were prepared using a very simple method; the gelator (Span 60 or Span 40) and the fluid phase were mixed, heated until the gelator dissolved/dispersed in the latter, followed by cooling of the sol phase. At gelator concentrations above a minimum (minimum gelation concentration, mgc, Table I), the sol phase set to an opaque, smooth, semi-solid gel as it cooled to room temperature. The color of the gel depends on the starting materials and is usually lighter in shade than the solvent. Span 40 and Span 60 are good gelators of all the nonionic surfactants shown in Table I, especially of Span 20 and of Tween 40; the low minimum gelation concentration of these gels means a large number of solvent molecules are immobilized per gelator molecule; for example, in 7% w/w Sp60/Tw40, approximately five solvent molecules are immobilized per gelator molecule. Span 60 is a better gelator as evidenced by its lower minimum gelation concentration compared to Span 40. The amphiphilogels are also thermoreversible: upon heating, the gel melts to the sol phase that can be cooled again to the gel state.

### Gel Microstructure

Light microscopy revealed that, like Span 60 and Span 40 organogels (5,12), Span 60 and Span 40 amphiphilogels consist of tubules that become more numerous with increasing gelator concentration. The tubules are clustered into star- or flower-shaped structures with a diameter ca. 10–50  $\mu\text{m}$ , depending on the gel (Fig. 1). The clusters, dispersed throughout the continuous phase, are linked to one another forming a coherent network. Electron microscopy showed more clearly that the star-shaped clusters are composed of tubules that appeared to have a central "node" and that the tubular

**Table I.** Minimum Gelation Concentrations for the Formation of Amphiphilogels Containing Span 40 or Span 60 as Gelators

Solvent	Minimum gelation concentration (% w/w)	
	Span 40 (Sorbitan monopalmitate) [6.7]	Span 60 (Sorbitan monostearate) [4.7]
Tween 20 (Polysorbate 20) [16.7]	18	15
Tween 40 (Polysorbate 40) [15.6]	7	4
Tween 80 (Polysorbate 80) [15.0]	20	20
Tween 85 (Polysorbate 85) [11.0]	19	15
Span 20 (Sorbitan monolaurate) [8.6]	7	9
Span 80 (Sorbitan monooleate) [4.3]	> 30	20
Span 85 (Sorbitan trioleate) [1.8]	20	20

HLB values for the surfactants are shown in [ ].

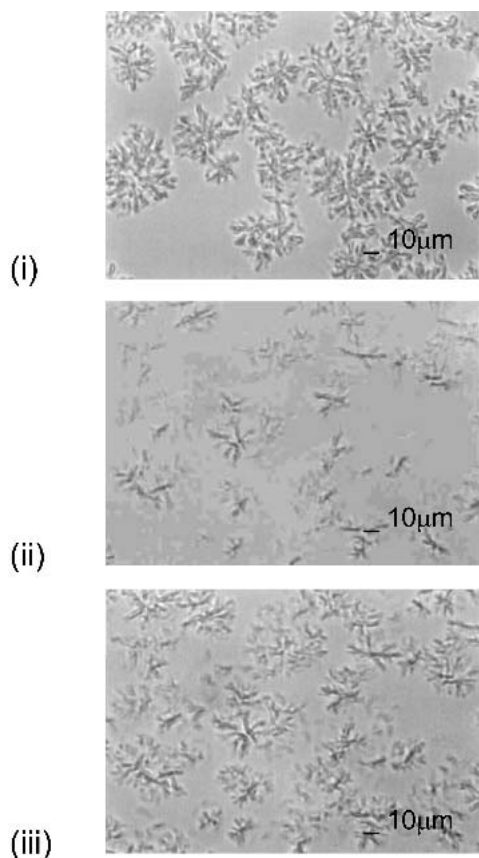


**Fig. 1.** Light micrographs of 20% w/w Span 60 in Span 85 amphiphilgel, taken on a hot stage. (i) At room temperature; (ii) the gel has been heated to 60°C then cooled to 40°C; (iii) the gel has been further cooled to 30°C. Clusters of tubules form a 3D network and immobilize the fluid phase. Increasing the temperature causes the microstructure to disappear as the gelator network dissolves in the solvent. The gel reforms as the temperature falls below the gelation temperature and tubular clusters appear (ii, iii).

aggregates are linked to others via junction points (Fig. 2). In contrast to the star-shaped clusters of tubules in the majority of the amphiphilgels, the microstructures of certain gels, for example where Tween 60 or Span 20 is the fluid phase, consist of longer tubular fibers and short strands which grow in a uni-directional manner as the temperature of the system falls to below the gelation temperature (Fig. 3).

The thermoreversibility of the amphiphilgels is exhibited clearly under the light microscope; the clusters and tubules melt and dissolve back into the solvent when the gel is heated and reform when the sol phase is cooled (Fig. 1). As the temperature is increased, the larger clusters are the first to start melting, and reduce in size; eventually individual fibers/tubules are left and are the last to disappear. Cooling the sol phase results in the reappearance of the tubules and clusters; the latter grow radially from a central “node.”

To probe gel microstructures in greater detail, SANS experiments were conducted. The scattering spectrum of 10% D-Sp60/H-Tw80 system as it was heated to 50°C then cooled again to the gel state is shown in Fig. 4. The spectra show a high scattering in the low  $Q$  range in gels at 20–48°C, which disappears at 50°C. A Bragg peak at approximately  $12\text{Å}^{-1}$  can be seen at 20°C, that disappears upon heating, and

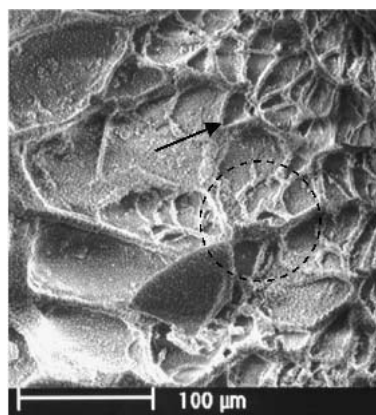


**Fig. 2.** Scanning electron micrograph of a 20% w/w Span 40 in Tween 80 amphiphilgel. Numerous fibers can clearly be seen, meeting at junction points (arrow) which confer rigidity and stability to the structure. The organization of tubules in star-shaped clusters is also visible as shown by the dotted lines.

appears once again when the gel phase was cooled back to 20°C (Fig. 4).

### Phase Transition Temperature

Phase transition temperature was measured using three different techniques: hot stage microscopy, melting point apparatus, and HSDSC (Figs. 5–7).

The gels were observed using hot-stage light microscopy, as they were heated and cooled. Upon heating, the tubular clusters disappeared: the supramolecular architecture melted and gelator molecules dissolved/dispersed in the bulk solution, and the sol phase was obtained. Upon cooling, the clusters reformed, as shown in Fig. 1, reflecting the gels' thermoreversibility. Gel melting on the hot stage microscope occurred over a broad temperature range (of approximately 5°C) which corresponds to the time at which the clusters or strands of tubules started to melt, until they disappeared altogether. The HSDSC trace also shows a fairly broad phase transition temperature (Fig. 7). The transition temperature increased as gelator concentration was increased (Fig. 5). Furthermore, at the same gelator concentration, the melting points of both Span 60 and Span 40 gels increased with increasing HLB of the liquid component of the gel.

HSDSC—an objective method—was also used to measure the transition temperature ( $T$ ) of some of the gels as these were heated and cooled back to the gel state (Figs. 6 and 7). HSDSC gave consistently lower transition temperatures

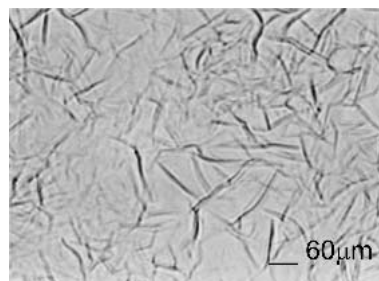


**Fig. 3.** Light micrographs of 1% w/w Span 60 in Tween 60 amphiphilgel. The amphiphilgel contains tubular fibers of gelator throughout the continuous phase, rather than clusters.

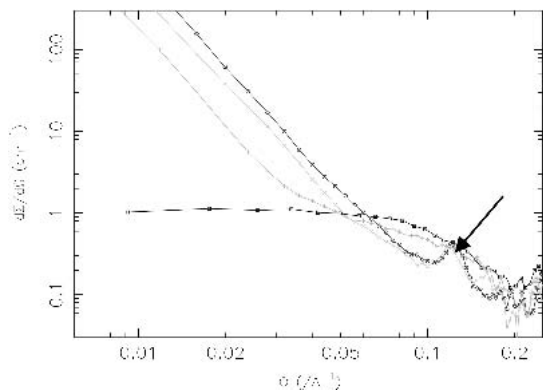


**Fig. 4.** SANS graph of 10% w/w D-Span 60 in H-Tween 80 amphiphilgel as it was heated from 20°C to 60°C and back again. ○, 20°C, □, 50°C, +, 48°C, ×, 20°C after heating. Arrow indicated Bragg peak at 20°C.

than hot-stage microscopy and the melting point apparatus. The transition temperature obtained on heating the gel was higher than the T value obtained when the resulting sol phase was cooled. For example, a peak at 33.5°C was obtained when heating 20%Sp40/Tw80 gel, but during the cooling phase, the gelation peak appeared at 26.9°C (Fig. 7). Similarly, the phase transition temperature of 20%Sp60/Sp80 gel was found to be 33.3°C upon heating the gel, but 26.2°C upon cooling the sol phase.

Storing the gels for 2 years at room temperature in closed vessels resulted in a slight, but significant, increase in the T of certain gels (Table II).

**Gel Lifetime**

All the amphiphilgels, except for Span 40 in Span 85, shown in Table I had lifetimes of more than 2 years at room temperature. Span 40 in Span 85 gel syneresed after 6 months of storage.

**Gel Flow Properties**

A typical example of a flow diagram of one of the amphiphilgels tested is shown in Fig. 8. Under shear, which reached up to 700 s<sup>-1</sup> in some gels, the viscosity of all gels fell considerably, with the viscosity of some becoming equivalent to that of glycerol (e.g., 1.3 Pa.s for 20% w/w Span 60 in

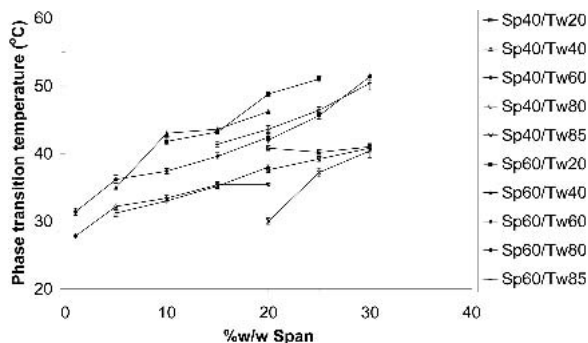


**Fig. 5.** Phase transition temperatures (T) of Span 60 and Span 40 gels measured by the melting point apparatus (mean ± SEM). Melting points of Span 60 = 55.2 ± 0.6°C; melting point of Span 40 = 47.8 ± 0.4°C.

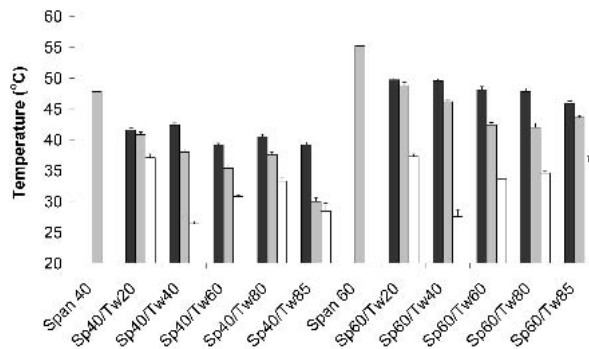


**Fig. 6.** Comparison of phase transitions temperatures of 20% w/w Span 40 or 20% w/w Span 60 in Tween gels, using the hot stage microscope (black), melting points apparatus (gray), and HSDSC (white); values are mean ± SEM.

Tween 80). In addition, all the gels exhibited a hysteresis loop. Certain gels (e.g., Span in Tween 40, or in Span 20) exhibited a yield point, that is, shear stress that must be exceeded before the gel will flow. When the gelator was present at 30% w/w, all the gels tested showed a yield point corresponding to a hard gel consistency. Increasing gelator concentration leads to a significant increase in the zero-rate viscosity of Span 60 amphiphilgels (Fig. 9) (p < 0.05). The minimum gelator concentration needed for a gel to have a yield point depended on the gelator—20%Sp60/Tw85 gel demonstrated a yield point, but 20%Sp40/Tw85 did not. At any one gelator concentration, a significant difference was

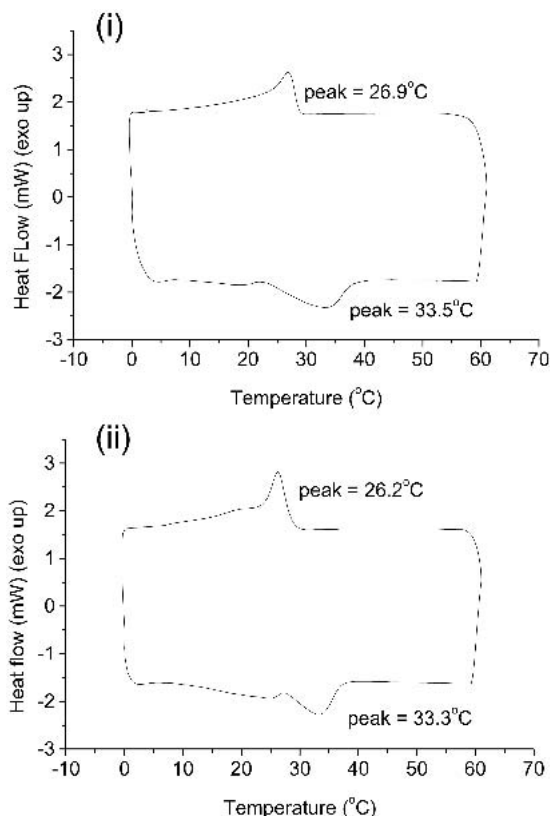


**Fig. 7.** HSDSC traces of (i) 20%Sp40/Tw80 and (ii) 20%Sp60/Tw80 during heating from 0 to 60°C and back to 0°C at a rate of 1°C/min.

**Table II.** Phase Transition Temperatures (T) of 20% w/w Span 60 or Span 40 Gels When Prepared Fresh and After 2 Years Storage

Amphiphilgel (20% w/w gelator)	T when prepared fresh (°C)	T after 2 years storage (°C)
Sp40/Tw20	40.8 ± 0.4	41.6 ± 0.5
Sp40/Tw40	38.0 ± 0.3	41.2 ± 0.6 <sup>a</sup>
Sp40/Tw60	35.4 ± 0.2	37.0 ± 0.9
Sp40/Tw80	37.6 ± 0.4	38.0 ± 0.7
Sp40/Tw85	30.0 ± 0.4	32.6 ± 0.7 <sup>a</sup>
Sp40/Sp20	33.6 ± 0.5	34.4 ± 0.8
Sp60/Tw20	48.8 ± 0.4	51.8 ± 0.9 <sup>a</sup>
Sp60/Tw40	46.2 ± 0.4	50.0 ± 0.4 <sup>a</sup>
Sp60/Tw60	42.4 ± 0.5	43.8 ± 0.8
Sp60/Tw80	42.0 ± 0.5	44.2 ± 0.7 <sup>a</sup>
Sp60/Tw85	43.6 ± 0.5	46.0 ± 0.7 <sup>a</sup>
Sp60/Sp20	39.6 ± 0.5	41.2 ± 0.8
Sp60/Sp80	37.4 ± 0.7	39.4 ± 0.5
Sp60/Sp85	48.8 ± 0.7	51.0 ± 0.7

<sup>a</sup> p < 0.05 compared to fresh.

found between the zero-rate viscosities of the gels containing different fluid phases (p < 0.001, Fig. 9).

Age affected the different amphiphilogs in different ways, although all the gels were still thixotropic. No difference was found in the viscosities of all the gels after 1, 6, and 12 months of storage. Most gels had no significant change in viscosity even after two years storage (p > 0.05). In addition, no difference could be seen in the microstructure of the gels when viewed under the light microscope. However, amphiphilogs composed of 20% w/w gelator in Tween 20 or Tween 80 had higher viscosities following storage for 2 years (Table III), in addition to exhibiting a yield value which was absent in freshly prepared gels. A stronger gel network was not always formed with time however. Gels composed of 20% w/w gelator in Tween 40 and 20%Sp60/Tw85 still exhibited a yield point after 2 years, but the zero-rate viscosity decreased, whereas 20% w/w gelator in Span 20 had lost its yield point following storage over two years, and the zero-rate viscosity also decreased.

All amphiphilogs showed reduced viscosity with increasing temperature (Table III). The rheograms of most of the gels did not show a hysteresis loop at 45°C. The viscosities of 20%Sp60/Tw20 and 20%Sp60/Sp85 did not decrease sig-

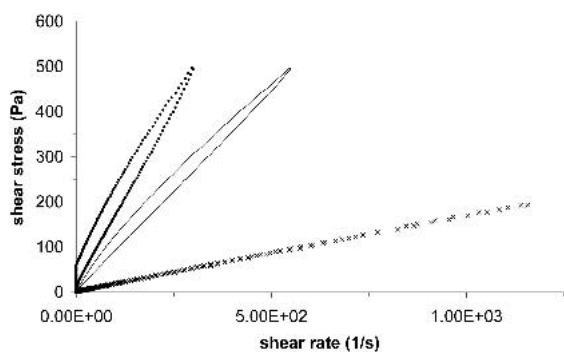


**Fig. 8.** Flow rheogram of 20% w/w Span 60 in Tween 80 amphiphilgel at room temperature (—), at 2 years old (○), and at 45°C (●). The 2-year-old gel has a yield point at approximately 25 Pa; shear-thinning properties were not present at 45°C, as the amphiphilgel had melted into the sol phase at that temperature.

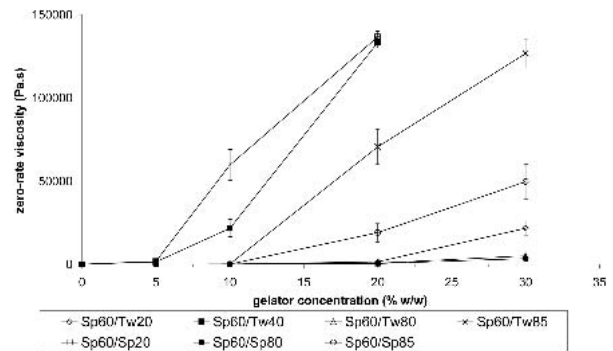


**Fig. 9.** The effect of gelator concentration on zero-rate viscosity of the amphiphilogs [mean (n = 3) ± SD].

nificantly when the temperature was increased to 45°C, and a hysteresis loop was still present in the rheograms.

## DISCUSSION

### Gel Formation and Minimum Gelation Concentration

Gel formation occurs when the sol phase is cooled, as the gelator solubility in the solvent is reduced, resulting in reduced gelator-solvent affinity and self-assembly of gelator molecules into tubular structures which form a coherent network throughout the fluid phase, thus immobilizing it. The amphiphilogs, which are held by physical interactions, can be regarded as physical gels, as defined by Terech (13).

Span 60 tends to form gels at slightly lower concentrations than Span 40 (Table I). The only difference between the two gelators is that Span 60 possesses a longer hydrocarbon (lipophilic) chain, by two carbons, in its chemical structure. The greater lipophilicity of Span 60 (HLB 4.7 vs. 6.7 for Span 40) is bound to affect gelator-solvent affinities, and ultimately gelator self-assembly which leads to gelation. The longer hydrocarbon chain in Span 60 may also enable a greater number of hydrophobic interactions that stabilize the gelator assemblies which increases the likelihood of gel formation at lower gelator concentrations. The difference in minimum gelator

**Table III.** Zero-Rate Viscosities of 20% w/w Span 60 in Span or in Tween Amphiphilogs, at 25°C, 32°C, and 45°C, and After 2 Years Storage in Closed Vials

Gel	Zero-rate viscosity (mean ± SEM,) (10 <sup>3</sup> Pa) at		
	25°C	32°C	45°C
Sp60/Tw20	1.50 ± 0.200	1.05 ± 0.302	0.461 ± 0.205
2 years old	11.3 ± 0.700	ND	ND
Sp60/Tw40	133.3 ± 3.33	1.23 ± 0.180	0.006 ± 0.0004
2 years old	69.0 ± 5.86	ND	ND
Sp60/Tw80	0.677 ± 0.342	0.220 ± 0.095	0.004 ± 0.001
2 years old	20.3 ± 4.91	ND	ND
Sp60/Tw85	97.7 ± 36.6	0.890 ± 0.064	0.019 ± 0.013
2 years old	9.70 ± 0.21	ND	ND
Sp60/Sp20	136.7 ± 3.33	1.97 ± 0.285	0.0007 ± 0.333
2 years old	53.3 ± 20.9	ND	ND
Sp60/Sp80	0.433 ± 0.100	0.216 ± 0.070	0.0003 ± 0.333
2 years old	0.667 ± 0.170	ND	ND
Sp60/Sp85	17.6 ± 6.25	5.77 ± 1.43	2.17 ± 1.21
2 years old	40.3 ± 7.97	ND	ND

concentrations of Span 60 and Span 40 may also be explained by the different solubilities of the two gelators in the fluid phase; the higher melting point of Span 60 (55.2°C compared to 47.8°C of Span 40) indicates that solubility of Span 60 in the fluid phase might be lower, as more energy is needed to break the solute-solute bonds, when the cavity model of solute dissolution is considered (14). A lower solubility of the gelator in the fluid phase would result in lower solvent-gelator interactions as the sol phase is cooled and, ultimately, gelator self-assembly at lower concentrations. Span 60 and Span 40 are known to behave differently when used to gel organic solvents (12). It is also known that small changes in gelator structure can have a large impact on other organogels (15). Nuclear magnetic resonance or mass spectrometry may help to elucidate the molecular interactions that occur upon gelation, and the orientation of the molecules with respect to each other, which would explain the relatively large effects caused by an extra ethyl group in Span 60 compared to Span 40.

From Table I, we can see that there was no correlation between ease of gelation (mgc) and nature of the solvent. One could have expected easier gelation in solvents that are dissimilar in polarity to the gelator, which would result in reduced gelator-solvent and increased gelator-gelator interactions, and a greater likelihood of gelation. This, however, did not happen. The liquid Spans (more similar to the gelators) could be gelled as easily as the Tweens. This indicates that an estimation of relative insolubility of the gelator in the fluid phase (as predicted by the "like dissolves like" adage (16) can not be used to predict gelation, that is, solubility of gelator in solvent does not necessarily lead to absence of gelation and *vice versa*.

### Gel Microstructure

The gelator molecules aggregate together as the temperature of the sol phase is reduced (Fig. 1), and form tubular structures that join together at junction points to form interconnected clusters throughout the continuous phase (Fig. 2). The junction points are thought to add rigidity to the gel systems as previously reported (2,17,18). The increase in the number of clusters with increasing gelator concentration confirms that the gelator is responsible for tubule and cluster formation and that the tubules are aggregates of the gelator, formed by the self-assembly of these molecules when they separate out of the sol phase upon cooling. When viewed under polarized light, the tubular aggregates exhibit crystallinity; this shows the existence of organization of gelator molecules within the aggregates. Surfactants are known to form lyotropic mesophases at high concentrations in aqueous and in non-aqueous solvents (19). In gels, such phases occur as a result of a fall in the solubility of the gelator in the solvent when the temperature is reduced. The occurrence of anisotropic liquid crystals and lyotropic phases has also been reported in other organogels (20–21).

The amphiphilogs consist of clusters of tubules, except when Tween 60 or Span 20 was the fluid phase. In these gels, the gelator assemblies did not cluster around a central "node," but were fiber-like. The viscous nature of the fluid phase (Tween 60 is a semisolid and Span 20 is a thick viscous liquid at room temperature) seems to prevent the radial growth of gelator aggregates into clusters and fibrils are formed instead.

The amphiphilogs are thermoreversible, as already mentioned. Increasing the temperature causes the gelator structures to dissolve back into the continuous phase (solvent). The 3D network is, thus, destroyed and a sol phase is formed. Cooling the sol phase results in a reformation of the gel network as gelator molecules come out of solution and the tubular aggregates grow once more. From Fig. 1, the new structures appear to be smaller in size compared to the original tubular assemblies. It is possible that more time is needed for the larger structures to grow. Another reason for the smaller tubular assemblies is that, upon cooling the sol phase under microscope observation, gel formation occurred between cover slips (Fig. 1, ii, iii) and the physical restriction could have hindered the growth of gelator structures.

According to the SANS data, the strong  $Q^{-4}$ , Porod, scatterer at small  $Q$  is characteristic of scattering from smooth, sharp interfaces as might be expected of the micrometer-sized structures in the gel. Close to the melting temperature, this scattering rapidly disappears to be replaced by a signal characteristic of small particles, of radii around 19 Å. Note that at fixed total volume fraction of aggregates the signal at zero  $Q$ ,  $I(Q = 0)$ , is proportional to the volume of individual aggregates in equation (1). Given the chemical formulae of the components,  $\Delta\vartheta$  in (1) can be calculated and the absolute SANS intensity should provide confirmation of volume fraction  $\phi$  of the scatterers, or knowing  $\phi$  one may check the composition of the scatterer from the apparent  $\Delta\vartheta$ . For the 50°C aggregates in Fig. 4, some simple model fitting for  $P(Q)$  of polydisperse spheres suggests that the observed signal would only account for 10–15% of the D-Span 60, perhaps indicative of a very high critical aggregation concentration (cac). The room temperature data are consistent with around 30% of the known amount of D-Span 60, indicative again of a high cac, or more likely in this case that the aggregates are not composed entirely of deuterated material. Further studies over a wider range of concentrations on a single system might help find the value of a cac.

Thermoreversibility is shown by the loss of scatter as the gel was heated to 50°C, followed by the return of scatter when the sol phase was cooled to 48°C and then to 20°C. The extent of scatter increases with cooling, such that the scattering curves move closer to the original curve of gel at 20°C. The fact that two 20°C curves are not totally superimposed may be due to the fact that insufficient time had been allowed for structure formation upon cooling. The presence of a Bragg peak at around 0.12 Å<sup>-1</sup> indicates the existence of a repeating unit in some part of the sample with a D-spacing,  $2\pi/Q$ , of approximately 52 Å. The Bragg peak also disappeared at higher temperatures, confirming the absence of long-range gelator structures when the gel is melted to a sol phase. Interestingly, the Bragg peak was not present in the spectra of gels at 48°C even though there was a large amount of scattering at low  $Q$ . This is probably because the larger structures tend to dissolve in the fluid phase as temperature is increasing, and that is followed by the melting of the smaller tubular structures at higher temperatures. Such an observation is consistent with the hot stage microscopy results. The Bragg peak shows that the Span 60 tubules (shown in Figs. 1–3) are composed, at least in part, of lamellar repeat units with spacings of around 50 Å. One possible model for the organization of the lamellae within the tubules is a multilayer stack (sheets) (Fig. 10), where each layer (composed mainly of gelator) is 40 Å

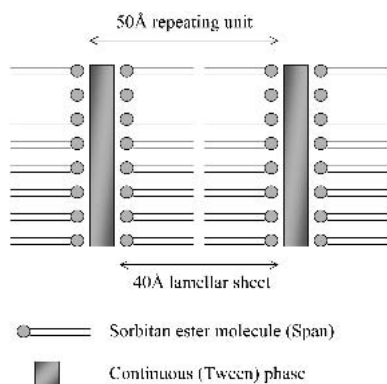


**Fig. 10.** Schematic diagram shows the organization of the gelator molecules into lamellar sheets in the tubular assemblies. Some of the liquid component is present between gelator lamellae.

thick, and is separated from the adjacent layer by fluid phase (Tween), to give a D-spacing of 50Å, evident by the presence of the Bragg peak as described earlier. Scattering contrast  $\Delta\delta$  for the Bragg peak comes from packing density variations, so the peak is also seen in H-Span/H-Tween samples with a similar intensity, but at slightly smaller Q, indicating a larger D-spacing.

Similar results were obtained with D-Span 60 in H-Tween 20. Addition of 1% w/w  $D_2O$  to D-Span 60/H-Tween 20 reduced the scattering signal, but addition of 1% w/w  $H_2O$  had no effect. Water added to the gel is expected to be incorporated in the hydrophilic portion of the gel, which is the Tween. The strength of the scattering signal obtained is related to the density contrast of the scattering bodies within the sample. A reduction in the signal means the contrast has been reduced (e.g., of aggregates against fluid phase background). This was observed upon addition of  $D_2O$ , which would have been associated with the Tween in the sample. As the Span 60 was also deuterated, the reduction in the contrast means the  $D_2O$ , and hence Tween, and Span 60 formed different scattering bodies. A small increase in the scattering signal upon addition of normal water confirms this. This leads us to believe that the aggregates are predominantly made up of the gelator, Span 60.

### Phase Transition Temperature

The cohesion of the gel network is assumed to arise from the strength of cross-links between the aggregates in a gel (2). Gel to sol phase transitions involve breakdown of the cross-links, disaggregation of the gelator assemblies and dissolution of the gelator molecules back into the solvent. All these events do not happen simultaneously or at exactly the same temperature, which explains why phase transition temperatures of physical gels often occur over a short temperature range. In addition, different techniques of determining the transition temperature measure the energy associated with the different events occurring at the phase transition and thus give different results. A sharp T was not expected for the amphiphilogs, and was not obtained by any of the three methods used to determine T. Hot-stage microscope observation showed that some tubular clusters took longer to melt than others; this is probably due to the variable number of cross-links and junction points in the clusters. A T range of 3–5°C is a typical property of physical gels, but is still indica-

tive of a homogenous microstructure within the gel (13). The broad melting point of the amphiphilogs can also be attributed to the polydispersity of the raw materials. As mentioned earlier, the surfactants used in the gels are mixtures, such that Span 60 and Span 40 are mixtures of the two compounds rather than being a pure form of just one. The different melting points of these two surfactants (55.2°C and 47.8°C for Span 60 and Span 40, respectively) will contribute to the broad melting temperature range of the gels.

The solid-to-liquid phase transition temperature of all amphiphilogs were below those of the gelator alone (55.2°C and 47.8°C for Span 60 and Span 40, respectively). This is a property of many organogels and is due to the fact that in the neat state, the gelator molecules are held together by strong intermolecular forces whereas, in the presence of the solvent molecules in the gel state, the gelator molecules may not pack into the same lattice and intermolecular forces between the gelator molecules are not as strong as they are in the solid state.

Increasing the gelator concentration led to an increase in phase transition temperature (Fig. 5), reflecting the more cohesive 3D network of gelator aggregates which immobilizes the fluid phase. Increasing the gelator concentration increases the number of gelator aggregates and the number of cross-links between aggregates such that more energy is required for the gel-to-sol transition.

The higher T with increased HLB of solvent reflects a stronger gelator network, and is probably due to higher gelator-gelator affinities compared to gelator-solvent affinities as the solvent HLB increases, i.e., as the solvent becomes more “different” to the lipophilic Spans, and as the gelator molecules become less soluble in the solvent resulting in a greater number of gelator aggregates and cross-links formed as the gelator molecules come out of solution upon gelation.

Although the Span 40 gels showed the same trends as the Span 60 gels, their transition temperatures were always slightly lower than the Span 60 gels (Fig. 5). This is probably due to the higher melting point of Span 60 gelator compared to Span 40 (55.2°C vs. 47.8°C). One could also suggest that the lower HLB of Span 60 (4.7 vs. 6.7) means that there is a greater difference between the HLB of the gelator and that of the Tween solvent, greater gelator-gelator affinities and a more robust 3D network. According to this hypothesis, a higher T would be expected for Span 40 in Span gels than the Span 60 in Span gels as the difference in HLB is greater in the former. However, this was not observed, which leads us to believe that the higher T of the Span 60 gels is most likely due to the higher melting point of Span 60 gelator.

The phase transition temperatures obtained by the different measurement techniques i.e., melting point apparatus, hot-stage microscopy and HSDSC, were compared. The melting point apparatus gave consistently lower values than the hot-stage microscope (Fig. 6). This is due to the fact that the former recorded the temperature at which the gels flowed (tubular aggregates may still be present), whereas the latter was used to record the temperature at which *all* the aggregates had melted. Indeed, phase transition temperatures of organogels are reported to be dependent on the physical techniques used to measure them, as the techniques measure different events at gelation (22–24). HSDSC gave even lower transition temperatures; this is probably because HSDSC can



record events that occur at lower temperatures and that are undetected by the naked eye, for example, disconnection of cluster-cluster and/or tubule-tubule junction points, perhaps by dissolution of some gelator molecules. The difference in  $T$  values obtained when heating and when cooling the gels during HSDSC (Fig. 7) can be explained by the fact that upon heating a gel, the tubular clusters detach from one another and decrease in size, followed by the melting of individual fibers/tubules until they all eventually disappear, as observed under hot stage light microscopy. Energy is required to overcome the forces of attraction between tubular clusters, between tubules, and between gelator molecules in the aggregates. In contrast, when the sol phase is cooled, tubular clusters grow outwards from a central nucleus. The growth of clusters may be occurring at a lower energy level, though we can not at present explain why this should be so. It is also likely that the lower  $T$  value during the cooling phase is linked to the formation of smaller gelator aggregates, as discussed earlier, and fewer or weaker junction points are initially formed between aggregates during the first few minutes of the cooling phase.

The increase in  $T$  following storage of the gels (Table II) is assigned to a greater number of and/or stronger junction points and thus, a stronger gel network being formed among tubular clusters over time. Such an effect on  $T$  over time, and the existence of different  $T$  values obtained upon heating a gel and cooling a sol phase have previously been reported for various physical gels (2,23).

### Gel Lifetime

Together with gelation temperature, gel lifetime is an indicator of gel stability (11,22). The fact that all but one of the tested gels had lifetimes greater than 2 years at room temperature is an indication of a stable gel network over a long duration. Syneresis is thought to be a result of the contraction of the solid network of tubules, as a result of which the fluid (that was initially trapped by the network) is pushed out and the two phases of the gel system separate. Syneresis is thought to be more likely in gels comprising larger aggregates (25). The larger pore size that exists between the large aggregates means that the fluid phase is not held so tightly within the gel network by capillary forces, and it can separate.

### Gel Flow Properties

The amphiphilogels' flow properties were investigated in an attempt to understand the nature of the gels and to determine how they would behave when applied topically onto the skin as a drug/vaccine delivery vehicle. The shear rate of rubbing formulations onto skin approaches  $10^5 \text{ s}^{-1}$  (26); it is, therefore, expected that the viscosities of the gels at such a shear rate would allow easy application onto skin as their viscosities fell with increasing shear. The hysteresis loop seen when the experiment was conducted at room temperature indicates that the gels demonstrate thixotropy; gel viscosity falls with applied shear rate, as the physical 3D network breaks up when the material is subjected to shear. When the sample was allowed to rest for some time, the 3D network structure reformed to a certain extent and many of the junction points were restored. The hysteresis loop shows that total structure recovery did not take place under the experimental

conditions. Such a flow profile is typical of many pharmaceutical systems such as creams, ointments and gels (27–32). Recovery of some structure, following the application of shear that is demonstrated by the amphiphilogels, is essential to ensure that the formulation will not flow off the site of application after administration. The yield point is an indication of the level of resistance to external forces before the system starts to flow and, thus, an indication of the strength of the gel network. The presence of a yield point with 20%Sp60/Tw85 and not with 20%Sp40/Tw85 reflects the stronger gelator network of the former gel, which is also evidenced in the higher phase transition temperature of this gel. Flow properties of the gels are influenced by parameters such as gel age, gelator concentration etc, as discussed below.

The increase in viscosity with increasing gelator concentration reflects the denser gelator network produced. The more robust 3D network traps and immobilizes the continuous phase to a greater degree, as a result of which, gel consistency, phase transition temperature and viscosity increase. As expected, a sharp rise in viscosity was observed once the minimum gelation concentration (mgc) had been reached (Fig. 9). Similarly, an increase in viscosity, or elastic modulus, with increasing gelator concentration has been reported for some organogels (17,33,34).

A significant difference was found between the viscosity of the gels containing different fluid phases. A major contribution to this is the different viscosities of the fluid phases. A viscous solvent, for example, Span 20, produced a gel with a harder consistency, a high viscosity, as well as a yield point at lower gelator concentrations, whereas less viscous solvents produced softer gels. This indicates the important contribution of the fluid phase toward the gel consistency.

Little change in the gel microstructure and consistency occurred over two years storage, except for gels composed of 20 gelator in Tween 20 or Tween 80 where the viscosity was found to increase following storage for 2 years (Table III). This indicates a stronger gel network formed with time; it is possible that more cross-links and junction points between the aggregates were established with time (2). Gels composed of 20% gelator in Tween 40 and the gel 20%Sp60/Tw85 had lower viscosities after two years, indicating some softening of the gel over time, and possibly structural breakdown.

Increasing the temperature at or above gel phase transition temperature resulted in melting of the aggregates network, dissolution of the gelator in the continuous phase, and the formation of a sol phase (a liquid) whose viscosity is considerably lower than that of the gel, and which does not show a hysteresis loop in the rheogram (Fig. 8). For gels whose phase transition temperature was well over  $45^\circ\text{C}$  (the highest temperature tested), for example 20%Sp60/Tw20 and 20%Sp60/Sp85 ( $48.8^\circ\text{C}$  and  $48.5^\circ\text{C}$ , respectively), increasing the temperature to  $45^\circ\text{C}$  did not result in a significant decrease in gel viscosity, and a hysteresis loop was still present in the rheograms, as these gels had not completely melted at that temperature. When the phase transition temperature was only slightly above the highest temperature tested (e.g. 20%Sp60/Tw40;  $T 46.2^\circ\text{C}$ ), increasing the temperature resulted in reduced viscosity as the gel started to melt and soften at  $45^\circ\text{C}$ . However, a hysteresis loop was still part of the rheogram due to the presence of gelator aggregates in the system at that temperature.

## CONCLUSIONS

In this paper, the preparation and characterization of opaque, thermoreversible, thixotropic amphiphilogs, composed solely of nonionic surfactants, has been described. Gelation occurs when the sol phase cools and gelator molecules self-assemble into tubular clusters or into long fibers which form a 3D network which immobilizes the fluid phase. The gelator structures are thought to consist of lamellar stacks of gelator molecules. A wide range of gels, where the gelator was either Span 60 or Span 40, and where the fluid phase was a liquid Span or Tween, were tested; Span 60 in Tween gels proved to be the most promising for drug/vaccine delivery applications. These gels are stable at room temperature, do not synerese when stored for over two years, have higher phase transition temperatures than the Span 40 gels, and can usually form gels at lower gelator concentrations. This reflects the higher stability of the Span 60 organogels (5). The amphiphilogs' viscosities are sufficiently high to maintain semi-solid properties at rest, but fall upon shearing and at high temperatures. This should facilitate usage and topical application onto skin.

## ACKNOWLEDGMENTS

The authors thank David McCarthy for help with the microscope, Duncan Craig and Helen McPhillips for the use of the HSDSC, and Prof R. K. Thomas at the Physical and Theoretical Chemistry Laboratory, Oxford University, for the synthesis of deuterated Span 60. Funding by the School of Pharmacy, University of London is acknowledged.

## REFERENCES

1. K. Almdal, J. Dyre, S. Hvidt, and O. Kramer. Towards a phenomenological definition of the term 'gel'. *Polym. Gels Netw.* **1**:5–17 (1993).
2. P. H. Hermans. Gels. In H.R. Kruyt (ed.), *Colloid Science, vol II*, Elsevier Publishing Company Inc, Amsterdam, 1949, pp. 483–651.
3. P. J. Flory. Introductory lecture. *Disc. Faraday Soc* **57**:7–18 (1974).
4. S. Murdan, J. Ford, and A. T. Florence. Novel surfactant-insurfactant amphiphilogs. *J. Pharm. Pharmacol.* **50**:151 (1998).
5. S. Murdan, G. Gregoriadis, and A. T. Florence. Novel sorbitan monostearate organogels. *J. Pharm. Sci.* **88**:608–614 (1999).
6. S. Murdan and T. Andrýsek. Novel amphiphilogs for the oral delivery of cyclosporine A. *Proceedings of the 30th Annual Meeting of the Controlled Release Society*, held in Glasgow, Scotland, Poster 708. (2003).
7. S. Murdan, P. Arunothayanun, J. Ford, and A. T. Florence. Amphiphiloge systems as oral delivery vehicles for cyclosporin A: preliminary *in vivo* results. *Proceedings of the Symposium on Lipid and Surfactant Dispersed Systems*, 237–238 (1999).
8. N. Jibry and S. Murdan. *In vivo* investigation, in mice and in man, into the irritation potential of novel amphiphilogs being studied as transdermal drug carriers. *Eur. J. Pharm. Biopharm.* (2004).
9. S. Ropuszynski and E. Sczema. The effect of catalysts on the synthesis of fatty acid esters of anhydrosorbitols (Spans). *Tenside Surf. Deterg.* **22**:190–192 (1985).
10. S. Ropuszynski and E. Sczema. Dehydration of D-sorbitol in the presence of sodium phosphates. *Tenside Surf. Deterg.* **27**:350–351 (1990).
11. R. Mukkamala and R. G. Weiss. Physical gelation of organic fluids by anthraquinone-steroid-based molecules. Structural features influencing the properties of gels. *Langmuir* **12**:1474–1482 (1996).
12. S. Murdan. Novel surfactant based organogels: their structures and potential as vaccine adjuvants. University of London (1998).
13. P. Terech. Kinetics of aggregation in a steroid derivative/cyclohexane gelifying system. *J. Coll. Interface Sci.* **107**:244–255 (1985).
14. J. H. Richards. Solubility and dissolution rate. In M.E. Aulton (ed.), *Pharmaceutics, the Science of Dosage Form Design*, Churchill Livingstone, New York, 1995, pp. 62–63.
15. Y.-C. Lin, B. Kachar, and R.G. Weiss. Novel family of gelators of organic fluids and the structure of their gels. *J. Am. Chem. Soc.* **111**:5542–5551 (1989).
16. K. C. James. *Solubility and Related Properties*, Marcel Dekker Inc, New York, 1986.
17. P. Terech, V. Rodriguez, J. D. Barnes, and G. B. McKenna. Organogels and aerogels of racemic and chiral 12-hydroxyoctadecanoic acid. *Langmuir* **10**:3406–3418 (1994).
18. P. Terech, I. Furman, and R. G. Weiss. Structures of organogels based upon cholesteryl 4-(2-anthryloxy)butanoate, a highly efficient luminescing gelator: neutron and X-ray small angle scattering investigations. *J. Phys. Chem.* **99**:9558–9566 (1995).
19. D. Attwood and A. T. Florence. *Surfactant Systems, Their Chemistry, Pharmacy, and Biology*, Chapman and Hall, London, 1983.
20. T. Tachibana, T. Mori, and K. Hori. Chiral mesophases of 12-hydroxyoctadecanoic acid in jelly and in the solid state I. A new type of lyotropic mesophase in jelly with organic solvents. *Bull. Chem. Soc. Jpn.* **53**:1714–1719 (1980).
21. S. Yamasaki and H. Tsutsumi. Microscopic studies of 1,3:2,4-di-*o*-benzylidene-D-sorbitol in ethylene glycol. *Bull. Chem. Soc. Jpn.* **67**:906–911 (1994).
22. D. J. Abdallah and R. G. Weiss. Organogels and low molecular mass organic gelators. *Adv. Mater.* **12**:1237–1247 (2000).
23. P. Terech and R. G. Weiss. Low molecular mass gelators of organic liquids and the properties of their gels. *Chem. Rev.* **97**:3133–3159 (1997).
24. P. Terech, C. Rossat, and F. Volino. On the measurement of phase transition temperatures in physical molecular organogels. *J. Coll. Interface Sci.* **227**:363–370 (2000).
25. J. B. Kayes. Disperse systems. In M. E. Aulton (ed.), *Pharmaceutics, the Science of Dosage Form Design*, Churchill Livingstone, London, 1995, pp. 81–118.
26. H. A. Barnes, J. F. Hutton, and K. Walters. *An Introduction to Rheology*, Elsevier Science, Amsterdam, 1989.
27. B. W. Barry and A. J. Grace. Grade variation in the rheology of white soft paraffin BP. *J. Pharm. Pharmacol.* **22**:147S–156S (1970).
28. S. S. Davis. Viscoelastic properties of pharmaceutical semisolids I: ointment bases. *J. Pharm. Sci.* **58**:412–418 (1969).
29. G. M. Eccleston. Structure and rheology of cetomacrogol creams: the influence of alcohol chain length and homologue composition. *J. Pharm. Pharmacol.* **29**:157–162 (1977).
30. D. S. Jones, A. D. Woolfson, and A. F. Brown. Textural analysis and flow rheometry of novel, bioadhesive antimicrobial oral gels. *Pharm. Res.* **14**:450–457 (1997).
31. D. S. Jones, A. F. Brown, and A. D. Woolfson. Rheological characterisation of bioadhesive, antimicrobial, semisolids designed for the treatment of periodontal diseases: transient and dynamic viscoelastic and continuous shear analysis. *J. Pharm. Sci.* **90**:1978–1990 (2001).
32. M. Korhonen, L. Hellen, and J. Hirvonen. and J. Yliruusi. Rheological properties of creams with four different surfactant combinations - effect of storage time and conditions. *Int. J. Pharm.* **221**:187–196 (2001).
33. P. Schurtenberger, R. Scartazzini, and P. L. Luisi. Viscoelastic properties of polymerlike reverse micelles. *Rheologica Acta* **28**:372–381 (1989).
34. V. J. Bujanowski, D. E. Katsoulis, and M. J. Ziemelis. Gelation of silicone fluids using cholesteryl esters as gelators. *J. Mater. Chem.* **4**:1181–1187 (1994).